



# Fabrication and characterization of pure and modified $\text{Co}_3\text{O}_4$ nanocatalyst and their application for photocatalytic degradation of eosine blue dye: a comparative study

Prashant Bhimrao Koli<sup>1</sup> · Kailas Haribhau Kapadnis<sup>2</sup> · Uday Gangadhar Deshpande<sup>1</sup> · Manohar Rajendra Patil<sup>3</sup>

Received: 14 September 2018 / Accepted: 16 November 2018 / Published online: 26 November 2018  
© The Author(s) 2018

## Abstract

The present work deals with the synthesis of cobalt oxide, and  $\text{Fe}^{2+}$ - and  $\text{Ni}^{2+}$ -doped cobalt oxide nanoparticles as a catalyst. The study is investigating the different factors in obtaining cobalt oxide, and  $\text{Fe}^{2+}$ - and  $\text{Ni}^{2+}$ -doped cobalt oxide nanoparticles. Photocatalytic degradation studies are carried out for water-soluble eosine blue (EB) dye using cobalt oxide, and  $\text{Fe}^{2+}$ - and  $\text{Ni}^{2+}$ -doped cobalt oxide nanoparticles in aqueous solution. Different parameters such as initial dye concentration, dose of catalyst, contact time and pH have been studied to optimize reaction conditions. It is observed that photocatalytic degradation is a more effective and faster mode of removing EB dye by cobalt oxide, and  $\text{Fe}^{2+}$ - and  $\text{Ni}^{2+}$ -doped cobalt oxide nanoparticles than work done before. The optimum conditions for the removal of the EB dye are initial concentration 40 mg/L, photocatalyst dose 0.8 g/L, and pH 7.5. The EDS technique gives the elemental composition of synthesised cobalt oxide, and  $\text{Fe}^{2+}$ - and  $\text{Ni}^{2+}$ -doped cobalt oxide nanoparticles. The TEM and XRD studies are carried for morphological feature characteristics of synthesised cobalt oxide, and  $\text{Fe}^{2+}$ - and  $\text{Ni}^{2+}$ -doped cobalt oxide nanoparticles. Pseudo-first-order kinetic has been investigated for both pure and doped cobalt oxide catalysts. Almost 95% dye degradation has been observed for doped cobalt oxide nanoparticles.

---

✉ Manohar Rajendra Patil  
profmanohar1985@gmail.com

Prashant Bhimrao Koli  
prashantkoli005@gmail.com

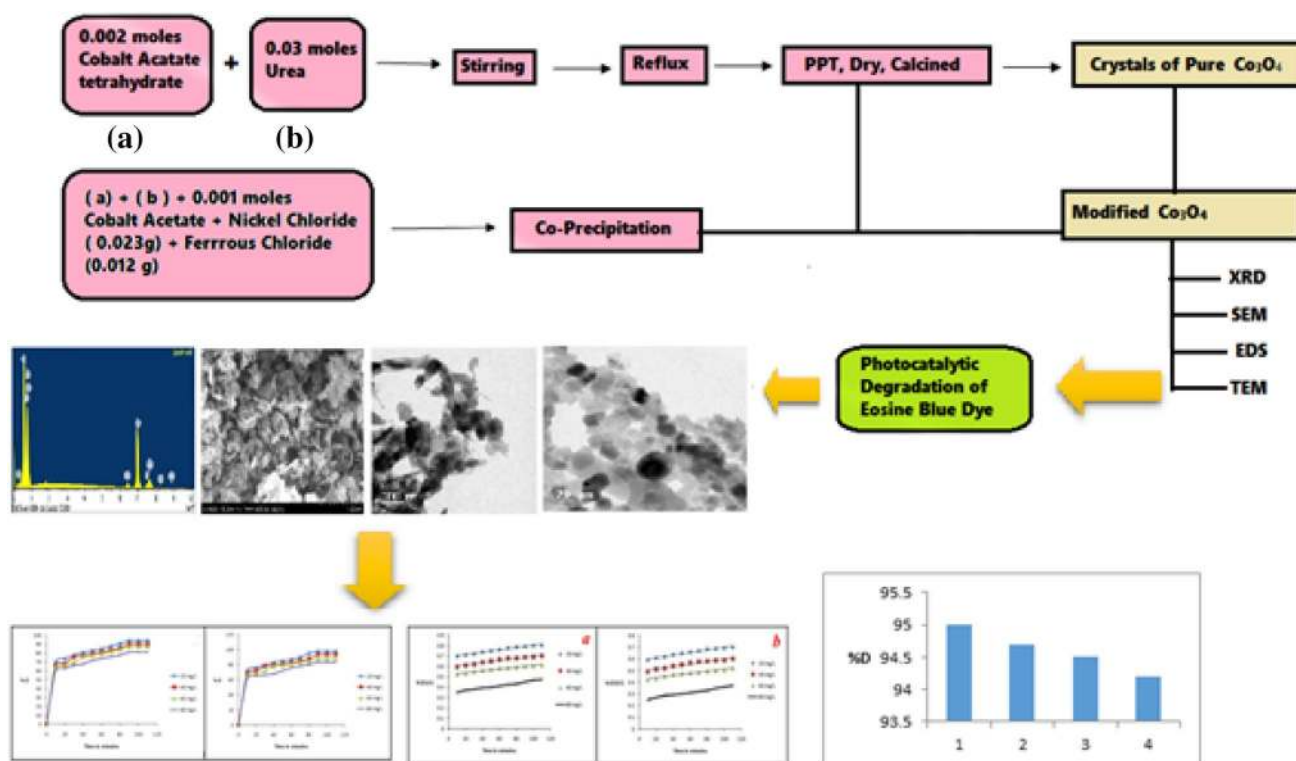
<sup>1</sup> Research Centre in Chemistry and PG Department of Chemistry, Pratap College of Arts, Science and Commerce, Affiliated to North Maharashtra University Jalgaon, Amalner, Jalgaon, MH 425401, India

<sup>2</sup> Research Centre in Chemistry and PG Department of Chemistry, Loknete Vyankatrao Hiray Arts, Science and Commerce College, Affiliated to SPPU, Panchavati, Nashik, Pune, MH 422003, India

<sup>3</sup> Nanochemistry Research Laboratory, Gajmal Tulshiram Patil Arts, Science and Commerce College, Affiliated to NMU, Nandurbar, Jalgaon, MH 425412, India



## Graphical abstract



Graphical abstract for photocatalytic degradation of eosine blue dye by cobalt oxide nanocatalyst.

**Keywords** Modified cobalt oxide nanoparticles · Eosine blue · Photocatalytic degradation · XRD · EDS · SEM · TEM

## Introduction

A huge number of strategies have been created to debase engineered colors from wastewater to diminish its affect on the environment. Over 70,000 tons of around 10,000 sorts of colors and shades are delivered every year around the world. About 20–30% colors are squandered in mechanical effluents amid the material coloring and wrapping up forms [1]. Colors and shades are broadly utilized, within the materials, plastics, calfskin and restorative industry to color items. The result of colored wastewater from these businesses may display an ecotoxic risk. Such colored gushing can influence photosynthetic forms of sea-going plants, diminishing oxygen levels in water and, in critical cases, coming about within the suffocation of sea-going vegetation and fauna. Most of the dyestuffs, counting azo colors, are poisonous and must be expelled over release into accepting streams since their effluents can diminish light entrance and photosynthesis [2]. Within the final decade, photocatalytic debasement forms have been broadly connected as strategies for the evacuation of natural poisons in wastewater and effluents, particularly the corruption of colors [3–11]. Among the unused oxidation strategies or progressed oxidation forms

(AOP), heterogeneous photocatalysis shows up as a rising removal technology driving to the whole purification of most of the natural toxins [12]. Semiconductor-mediated photocatalysis may be a well-established method for poison corruption. Photocatalysis could be a procedure which is carried by retention of light [13].

Cobalt-based nanoparticles are the most productive fabric for mechanical applications such as data capacity, attractive liquid and as a photocatalyst. Co is well-familiar ferromagnetic fabric which is commonly utilized as alloying component in lasting magnets. It comprises two shapes: hexagonal closed pressed (HCP) and confront centered cubic (FCC) [14, 15]. Co nanoparticles appear tall chemical reactivity, which makes them appropriate for catalysis. In case we need advance applications of cobalt in numerous businesses such as partition innovation, data capacity frameworks, catalysis and biomedicine, the nanoparticle is required to be depicted indistinguishable in measure, shape, uniform in composition and gem structure [16, 17].

Cobalt oxide nanoparticles are proficient semiconductor fabric for photocatalytic movement. Utilizing cobalt oxide, a few photocatalytic responses have been carried for the corruption of natural toxins such as colors. Cobalt oxide

nanoparticles have adequate band hole for the corruption of colors [18–21]. The doping in semiconductor fabric is one of the ways to extend their photocatalytic action. The aim behind doping is to alter the properties of nanoparticles to form a better catalyst. These type of advancement in the applications such as photocatalytic removal of several dyes is can be facilitated by doping of metals such as  $\text{Ni}^{2+}$   $\text{Co}^{2+}$  etc. [22, 23]. Uniform distribution of dopants in conjunction with an expansive surface zone and reasonably lower band crevice of a semiconductor fabric are crucial properties that unequivocally progress its photocatalytic properties. This cobalt oxide fabric is made indeed superior for corruption by doping it with  $\text{Fe}^{2+}$  and  $\text{Ni}^{2+}$  particles by utilizing appropriate forerunner. In this article, we have compared immaculate and doped cobalt oxide nanoparticle applications for the photocatalysis.

## Materials and methods

All chemicals used were analytical grade. The stock solution 1000 mg/L of dye was prepared in distilled water. 100 mL of dye solution of the desired concentrations was prepared from stock solution. In a first beaker, 100 mL of eosine blue dye solution of a desired concentration was taken, and cobalt oxide catalyst was added. Similar manner in a second beaker, 100 mL of eosine blue dye solution of a desired concentration was taken, and doped cobalt oxide catalyst was added. Both the dye solutions were irradiated with same mercury lamp to provide energy for excitation of cobalt oxide and doped cobalt oxide nanoparticles in the reactor. After the excitation of cobalt oxide and doped cobalt oxide nanoparticles, the degradation of dyes was studied using UV–Vis double-beam spectrophotometer. For that at the specific time intervals, suitable aliquot of the sample was taken from both the beaker and analyzed after centrifugation. The changes of dye concentrations were determined by UV–Vis double-beam spectrophotometer (Systronics model-2203) at  $\lambda_{\text{max}}$  530 nm in our laboratory.

## Experimental

### Procedure for the synthesis of $\text{Co}_3\text{O}_4$ nanocatalyst

0.5 g of cobalt acetate hexahydrate and 2.0 g of urea were dissolved in a 50 mL distilled water. After dissolution the pink colored solution was obtained. Then, the solution was stirred using a magnetic stirrer for 20 min to form a homogeneous solution. The resultant solution was transferred into the round bottom flask and the flask was connected to condenser and the solution was heated or refluxed for 12 h. After 12 h heating, the pink color of the solution changes to faint blue color and some solid crystals are formed. Cool

the solution at room temperature and filter. The residue was dried and transferred in the silica crucible and ignite for 7–8 h. After the complete ignition the black colored powder substance was obtained. Then the obtained product was placed in silica crucible in the muffle furnace at 600 °C for 6 h. Finally,  $\text{Co}_3\text{O}_4$  nanoparticles were prepared. Approximately 1 g of  $\text{Co}_3\text{O}_4$  was obtained by this process.

### Synthesis of modified cobalt oxide nanocatalyst

For the synthesis of doped cobalt oxide nanocatalyst, 0.45 g cobalt acetate, 0.012 g ferrous chloride, 0.023 g nickel chloride and 2 g urea were added to 80 mL of double distilled water and stirred on a magnetic stirrer for 20 min to form a pink color homogenous solution. Then, this solution was transferred to 100-mL round bottom flask and refluxed for 12 h. After cooling to room temperature, the obtained product was washed with distilled water and dried. The whole residue was calcined in a muffle furnace at 600 °C for 5 h.

## Results and discussion

### X-ray diffraction (XRD)

The XRD spectrum of pure and modified cobalt oxides are as shown below in Fig. 1a, b. Both pure and modified cobalt oxides were calcined at 600 °C, and analyzed by XRD with

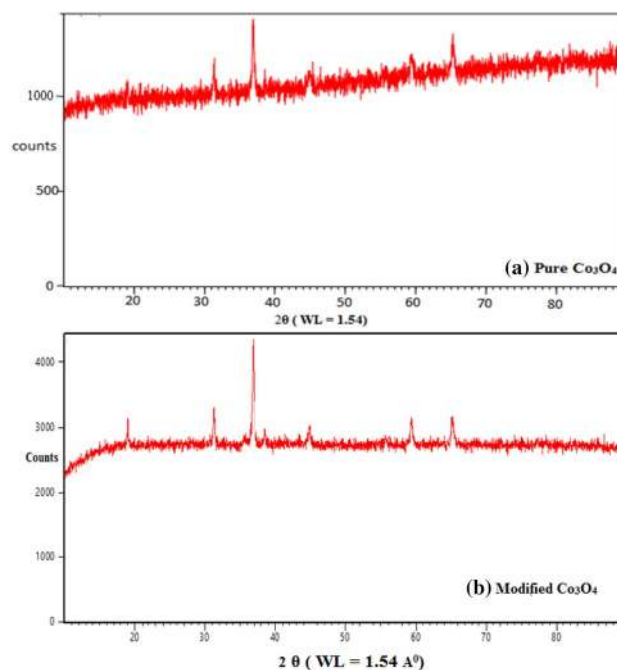


**Fig. 1** a XRD spectrum of pure  $\text{Co}_3\text{O}_4$ . b XRD spectrum of modified  $\text{Co}_3\text{O}_4$



model number X'Pert Pro equipped with X'Celerator solid-state detector along with Cu K-alpha-1 radiations. In the XRD spectrum of both these materials, no additional peaks were obtained indicating the formation of pure cobalt oxide material. The Bragg's diffraction peaks can be assigned to both the materials. In case of pure cobalt oxide, the diffraction peaks are obtained at 19.04, 31.32, 36.91, 44.90, 59.36, and 65.27, attributed to (111), (220), (311), (400), (422), and (440) planes, respectively. The cobalt oxide is a cubic material with the space group  $Fd\bar{3}m$  while it has lattice constant  $a=8.08 \text{ \AA}$ . The average particle size calculated from Scherrer's formula [ $D=K\lambda/\beta \cos\theta$ ], where  $D$  is the average particle size,  $K$  is constant (0.9–1),  $\beta$  is full width half maxima (FWHM) of diffracted peak, and  $\theta$  is the angle of diffraction. The average particle size for pure cobalt oxide was found to be 32 nm. The relative intensities obtained for pure cobalt oxide were matched with the JCPDS card number 073-1701. In the XRD data for modified cobalt oxide nanoparticles, the peaks reflected at 18.9977, 31.2489, 36.8327, 38.5208, 44.7909, 59.3170, and 65.1801. The average particle size calculated from Scherrer's formula for modified cobalt oxide was found to be 49 nm. The XRD spectrum is as shown in Fig. 1b.

## Scanning electron microscopy (SEM)

Scanning electron microscopy is widely used to study the morphological features and surface characteristics of catalyst surface. The pure and doped cobalt oxide nanoparticles are analyzed by SEM before photocatalytic degradation of eosine blue dye as shown in Fig. 2a, b. The SEM micrographs of pure and doped cobalt oxide nanoparticles show surface texture and porosity. It has heterogeneous-surfaced microspores and mesopores as seen from its surface micrographs. The random size of pure and doped cobalt oxide nanoparticles is 21.5 nm, 23.4 nm and 31.5 nm (Table 1).

The specific surface area of pure  $\text{Co}_3\text{O}_4$  and modified  $\text{Co}_3\text{O}_4$  nanoparticles were calculated using the BET method in the following equation:

$$S_w = \frac{6}{\rho x d}. \quad (1)$$

## Energy-dispersive spectroscopy (EDS)

Interaction of an electron beam with a test target produces an assortment of outflows. Energy dispersive spectroscopy (EDS) is utilized to allocate characteristic X-ray emissions portions into a huge range and EDS system program is utilized to separate the centrality keep running in driving force to pick the plenitude of particular fragments. EDS can be

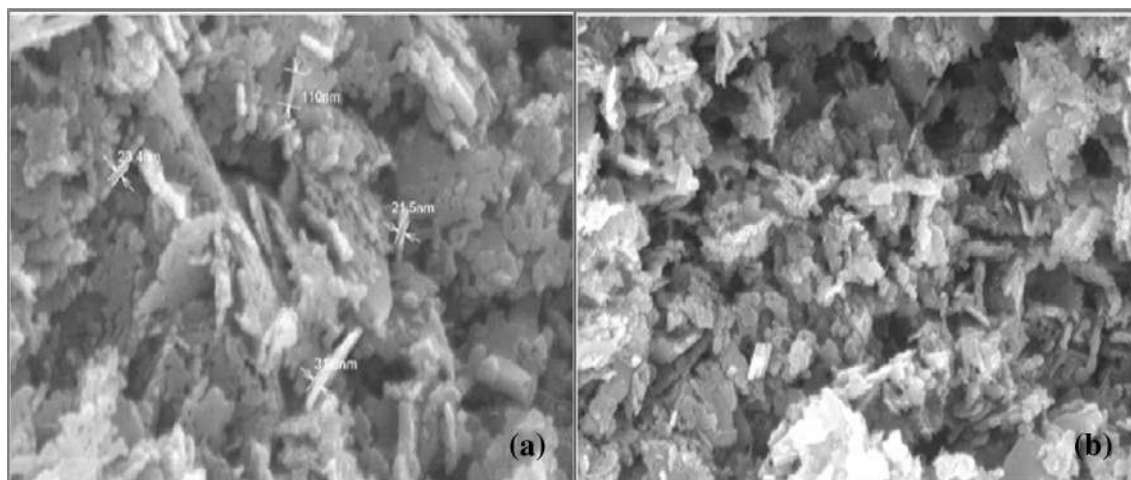


**Fig. 2** **a** SEM image of pure  $\text{Co}_3\text{O}_4$ , **b** SEM image of modified  $\text{Co}_3\text{O}_4$

**Table 1** Surface area and particle size calculated using BET method for spherical particles from SEM data

Functioning materials	Calcination temperature ( $^{\circ}\text{C}$ )	Crystallite (grain) size, $D$ (nm) (XRD)	Particle size, $d$ (nm) (SEM)	Specific surface area in $\text{m}^2/\text{g}$
Pure $\text{Co}_3\text{O}_4$	600	32.70	142.85	2.224
Modified $\text{Co}_3\text{O}_4$	600	49.49	200.0	3.068



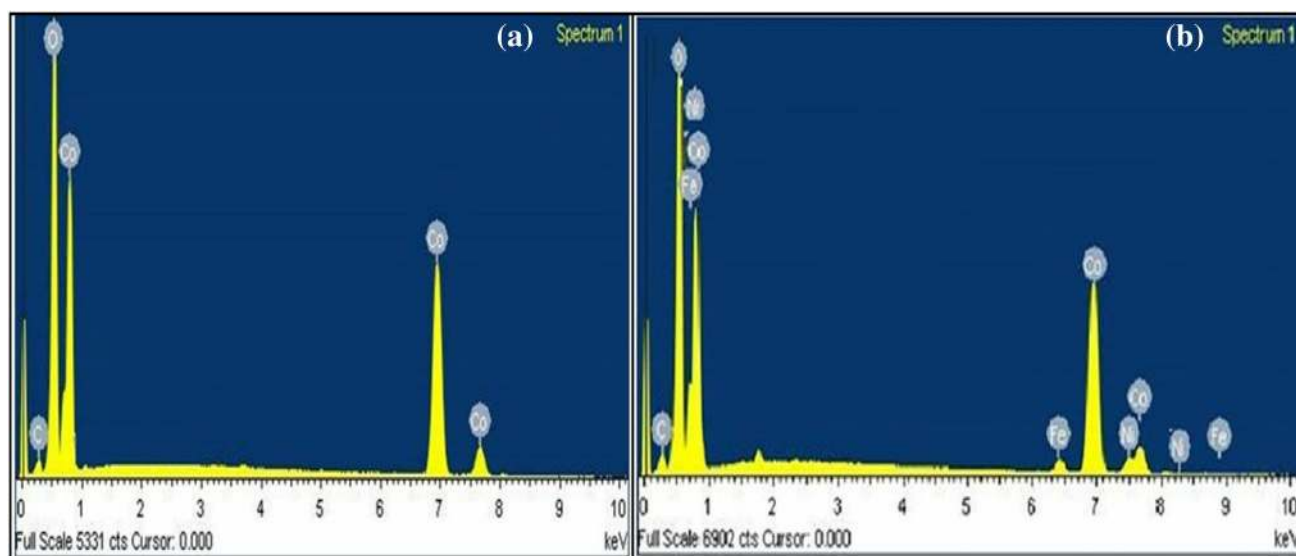


**Fig. 3** **a** EDS spectrum of pure  $\text{Co}_3\text{O}_4$ . **b** EDS spectrum of modified  $\text{Co}_3\text{O}_4$

**Table 2** Elemental composition of pure  $\text{Co}_3\text{O}_4$  nanoparticles

S. no.	Element	Series	Weight%	Atomic%
01	C	K	2.70	7.37
02	O	K	26.24	53.08
03	Co	K	71.05	39.36
04	Total		100.0	100.0

**Table 3** Elemental composition of modified  $\text{Co}_3\text{O}_4$  nanoparticles

S. no.	Element	Series	Weight%	Atomic%
01	C	K	2.93	8.07
02	O	K	24.60	50.88
03	Fe	K	4.79	3.05
04	Co	K	62.53	35.10
05	Ni	K	5.14	2.90
06	Total		100.0	100.0

utilized to discover the chemical composition of materials down to a spot estimation of a number of microns, and to make component composition maps over a much broader raster zone. Together, these capabilities give essential compositional data for a wide assortment of materials. The examination reveals that immaculate and doped cobalt oxide nanoparticles comprise correct natural composition of particular components in unadulterated cobalt oxide Co and O, whereas in doped cobalt oxide nanoparticles Fe, Ni, and Co appeared as within Fig. 3a, b (Tables 2, 3).

## Transmission electron microscopy (TEM)

To reveal the morphology and size of the synthesized particles, TEM images of pure cobalt oxide and modified cobalt oxide were recorded as shown in Fig. 4a–d. The particle size of the composite material ranges from 20 to 50 nm. The bright-field image of the nanoparticles shows the polycrystalline shape of the particles which are well dispersed with rough surfaces. Normally, the cobalt oxide crystal structure belongs to cubic system where the perfect cubes of pure cobalt oxide nanoparticles can be seen from the TEM images in Fig. 4a, b. The modified cobalt oxide also belongs to the cubic crystal system with the minute concentration of dopant in the cubic form which can be observed from TEM images in Fig. 4c, d.

## Selected area diffraction pattern (SAED)

Selected area diffraction pattern of pure and doped  $\text{Co}_3\text{O}_4$  nanoparticles is crystalline in shape as shown in Fig. 5a, b. Crystallinity of the sample is confirmed by the bright spots in the SAED Pattern. The diffraction data obtained from SAED are found to be in good agreement with the XRD data.

## Parametric study

The photocatalytic degradation of eosine blue dye was studied at  $\lambda_{\text{max}}$  530 nm. The optimum condition for removal of dye is 40 mg/L and pH 7.5 for pure  $\text{Co}_3\text{O}_4$  and doped  $\text{Co}_3\text{O}_4$  nanoparticles. The results obtained during this study are represented in Figs. 6, 7, 8, 9, 10.



**Fig. 4** **a, b** TEM images of pure  $\text{Co}_3\text{O}_4$ . **c, d** TEM images modified  $\text{Co}_3\text{O}_4$

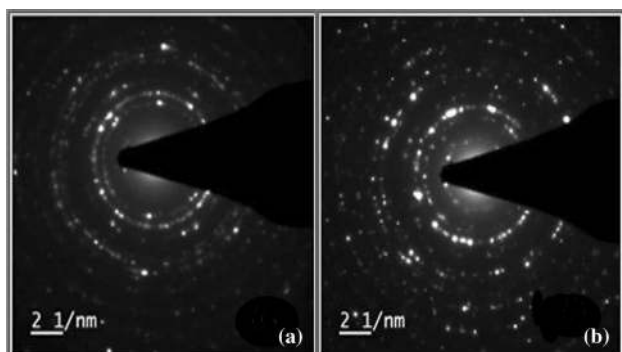
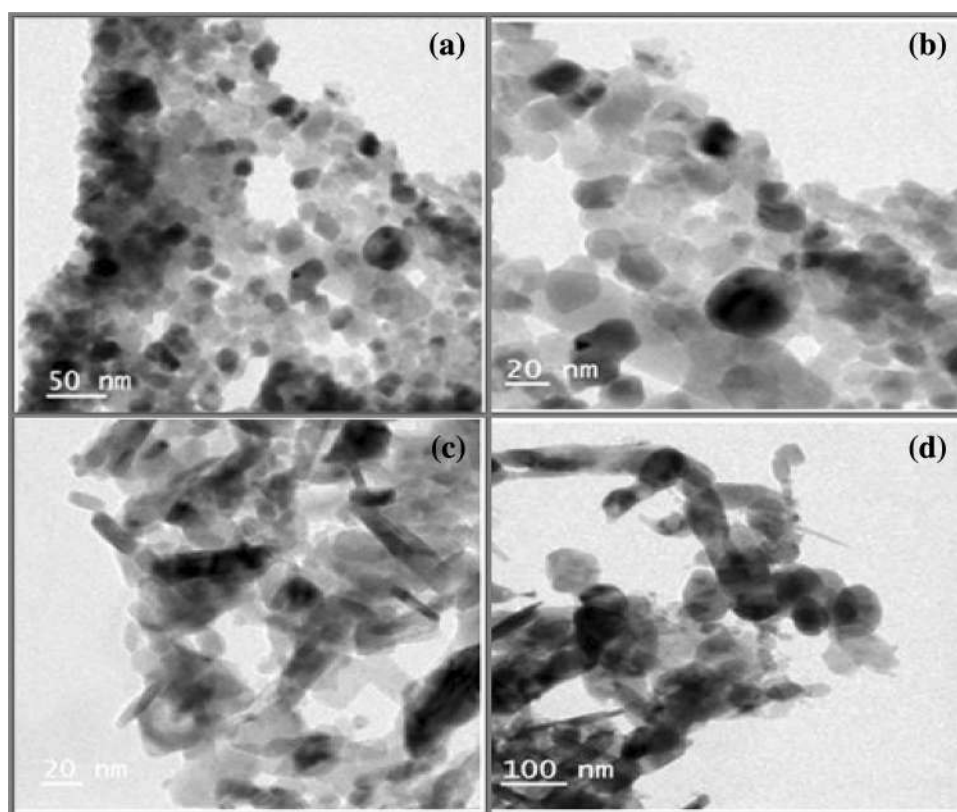


**Fig. 5** **a** SAED pattern of pure  $\text{Co}_3\text{O}_4$ . **b** SAED pattern of modified  $\text{Co}_3\text{O}_4$

#### Effect of catalyst dose

The effect of pure and doped cobalt oxide catalyst doses were studied on dye degradation when other experimental conditions for EB were studied at pH 7.5, and different dye concentrations for contact time 110 min were taken. The degradation percentage of EB dye by doped and pure cobalt oxide at different catalyst doses, 0.2–0.8 g/L for 20 mg/L, 40 mg/L, 60 mg/L and 80 mg/L of dye concentrations, were studied. It is observed that photocatalytic degradation of EB increases rapidly with an increasing amount of both pure and doped nano-cobalt oxide

catalysts. As the number of active sites of the catalyst increases, degradation of EB dye also increases as shown in Fig. 6a, b. The number of available active sites on the photocatalyst increases and hence an increase in the number of  $\cdot\text{OH}$  radicals produced which can take part in the degradation of the dye solution [24].

#### Effect of pH

The photocatalytic degradation of EB dye was studied at different pH values as it is an important parameter for reaction taking place on the particular surface. The role of pH in photocatalytic degradation of dye was studied in the pH range 0–12 at dye concentration 40 mg/L, and pure and doped cobalt oxide 0.8 g/L. It is observed that the rate of photocatalytic degradation enhanced with an increase in pH up to 7.5 as shown in Fig. 7a, b. The  $\text{pH}_{\text{PZC}}$  of the pure and doped cobalt oxide catalysts were estimated at about 7.5 using reported method [25]. The surface has net zero charge at  $\text{pH}_{\text{PZC}}$  and at  $\text{pH} > \text{pH}_{\text{PZC}}$ , the surface catalyst is negatively charged while  $\text{pH} < \text{pH}_{\text{PZC}}$  surface is positively charged. The maximum degradation of EB was obtained at pH 7.5 for both pure and doped cobalt oxide. The catalyst surface becomes negatively charged beyond pH 7.5 and EB dye was also in anionic form; hence, there was a strong repulsion observed between the dye molecule and catalyst



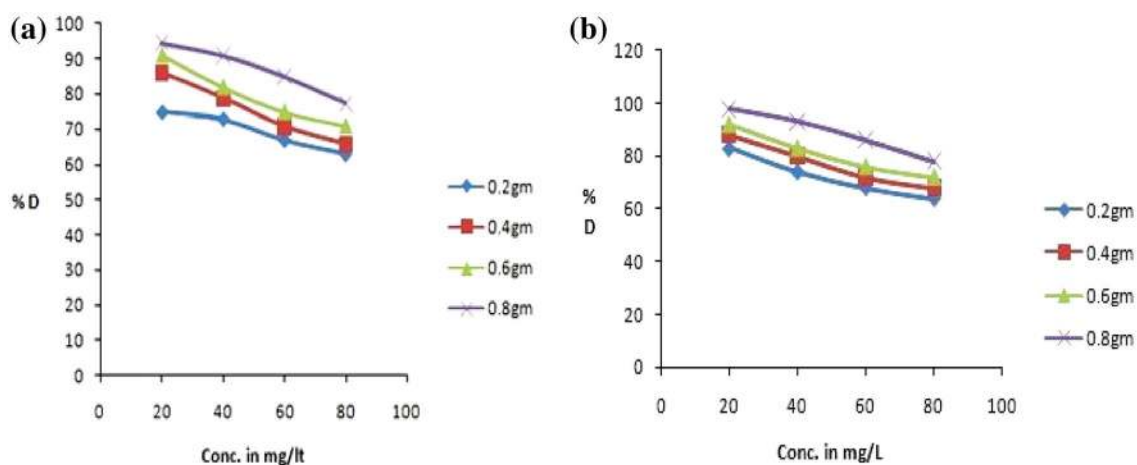


**Fig. 6 a** Effect of cobalt oxide catalyst dose on % degradation of eosine blue dye for different initial dye concentration with contact time 110 min, pH 7.5. **b** Effect of doped cobalt oxide catalyst dose on

% degradation of eosine blue dye for different initial dye conc. With contact time 110 min, pH 7.5

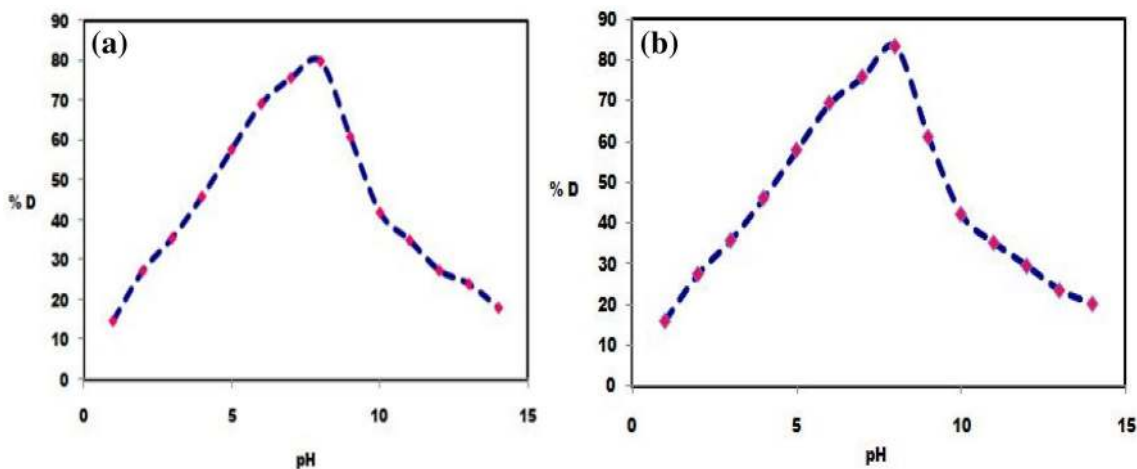


**Fig. 7 a** Effect of pH on degradation of eosine blue dye by pure cobalt oxide nanocatalyst. **b** Effect of pH on degradation of eosine blue dye by modified cobalt oxide nanocatalyst

surface. Consequently, the rate of degradation decreases for both pure and doped cobalt oxide nanocatalysts beyond pH 7.5.

#### Effect of contact time

The effect of contact time for the photocatalytic degradation of eosine blue dye by pure and doped cobalt oxide nanoparticles is shown in Fig. 8a, b. The dye was quickly degraded in first 20 min and then degradation rate continuously goes on increasing and reaches equilibrium in about 90 min. The rate of degradation of dye was initially fast because dye concentration was maximum; therefore, maximum amount of dye was adsorbed immediately and hence, the initial degradation rate was faster. As the maximum concentration of

dye was degraded from aqueous solution, the rate of degradation reaches at equilibrium. The rate of degradation of EB dye was maximum for doped cobalt oxide compared to pure cobalt oxide nanoparticles. The doped cobalt oxide has less band gap due to dopant  $\text{Fe}^{2+}$  and  $\text{Ni}^{2+}$  compared to pure cobalt oxide; hence, doped cobalt oxide was worked as a better photocatalyst for photocatalytic degradation of EB dye. The degradation of eosine blue can be explained on the basis of heterogeneous photocatalysis. This process involves generation of  $e^-$  and  $h^+$  which again generated  $\text{O}_2^-$  and  $^-\text{OH}$  radicals, respectively. These radicals are highly reactive and act as degrading agents. Moreover, photogenerated hydrogen atom from water is responsible for reductive degradation [25].

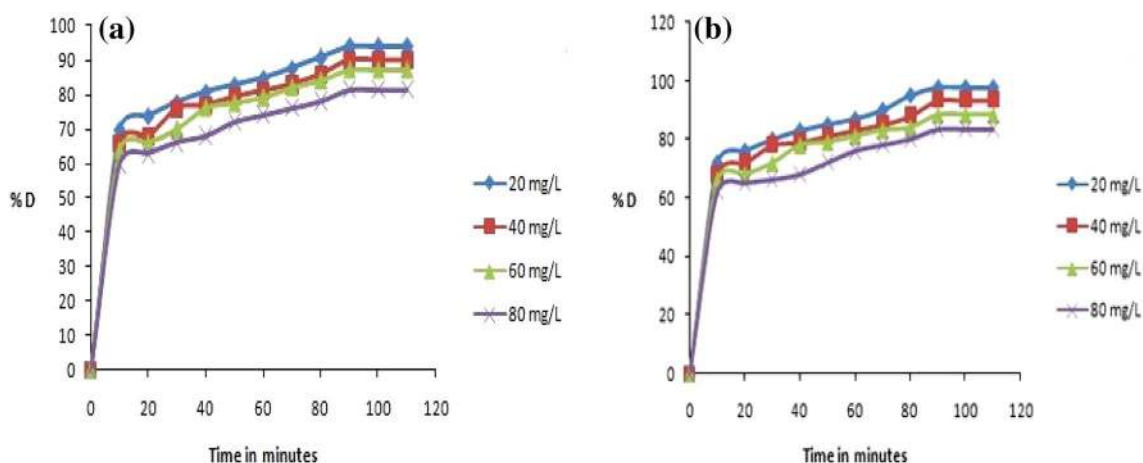


**Fig. 8** **a** Effect of contact time on % degradation of eosine blue dye at pure cobalt oxide catalyst dose 0.8 g/L at pH 7.5. **b** Effect of contact time on % degradation of eosine blue dye at modified cobalt oxide catalyst dose 0.8 g/L at pH 7.5

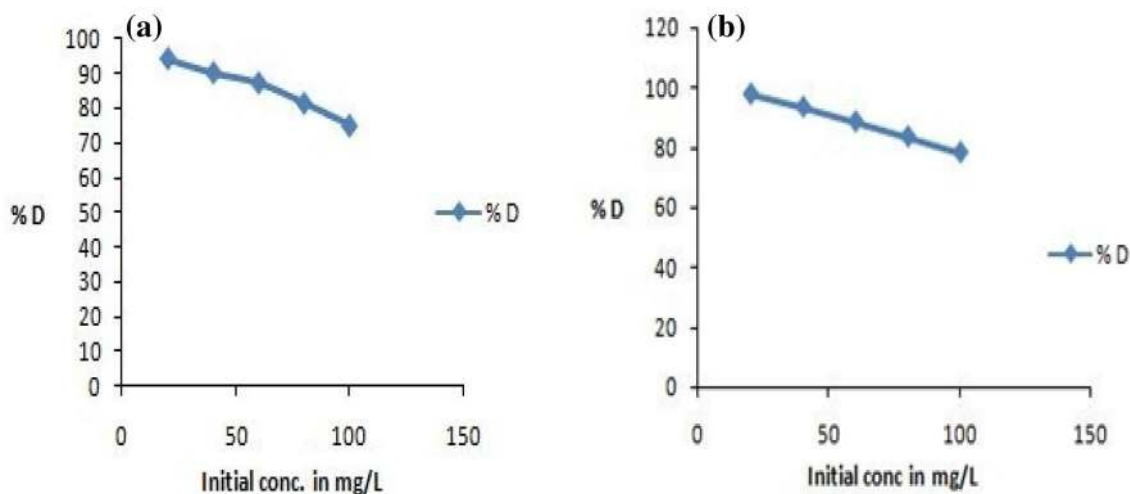


**Fig. 9** **a** Effect of initial dye concentration on % degradation of eosine blue dye by pure cobalt oxide catalyst dose 0.8 g/L at pH 7.5. **b** Effect of initial dye concentration on % degradation of eosine blue dye by doped cobalt oxide catalyst dose 0.8 g/L at pH 7.5

### Effect of initial dye concentration

The rate of degradation of EB dye was studied by varying the dye concentration from 10 to 100 mg/L. Because for fixed catalyst concentration active sites remains the same. With the increase of the initial EB concentrations, the EB molecules accumulate on the surface of pure and doped cobalt oxide catalysts. However, quenching between these excited eosine blue molecules irradiated by mercury light will take place. The quenching probability could also increase with the increase of the initial EB concentrations. Consequently, the photocatalytic efficiency of EB solutions was decreased with the increase of the initial EB concentrations. The

decrease in photocatalytic efficiency was maximum for pure cobalt oxide than doped cobalt oxide as shown in Fig. 9a, b. This was mainly due to decrease in band gap observed in doped cobalt oxide nanoparticles.

### Photocatalytic degradation kinetics study

**Pseudo-first order** The photocatalytic degradation of EB dye on the surface of pure and doped cobalt oxide follows pseudo-first-order kinetics. It can be expressed according to the pseudo-first-order equation, where  $C$  and  $C_0$  are the reactant concentration at time  $t=t$  and  $t=0$ , respectively, and  $k$  and  $t$  are the pseudo-first-order rate constant (reac-



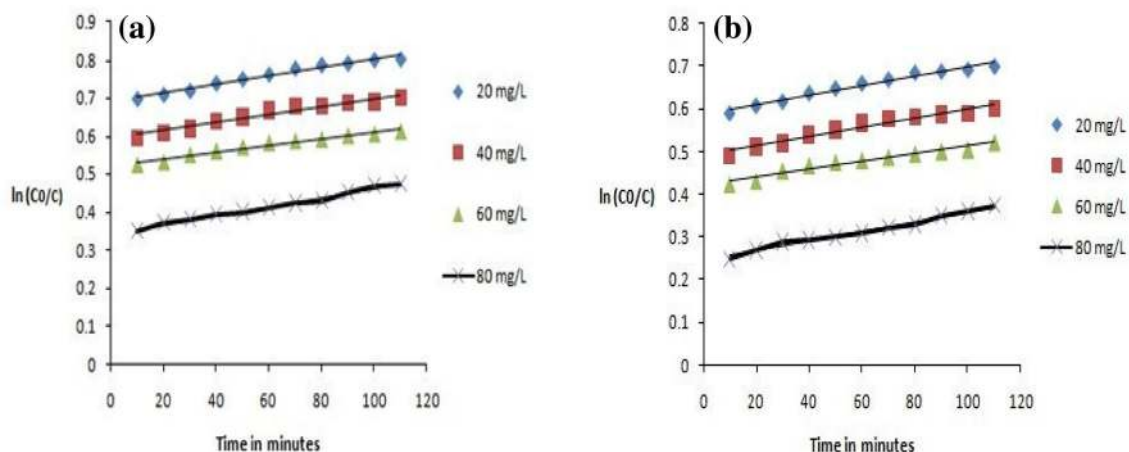


**Fig. 10** **a** Pseudo-first-order kinetics for photocatalytic degradation of eosine blue dye with pure cobalt oxide dose 0.8 g/L. **b** Pseudo-first-order kinetics for photocatalytic degradation of eosine blue dye with doped cobalt oxide dose 0.8 g/L

**Table 4** Reaction rate constant of EB photocatalytic degradation with different initial concentration for pure (a) and modified (b) cobalt oxide catalyst

Amount of catalyst	Initial concentration in mg/L	Rate constant ( $K$ )	$R^2$
(a) Pure cobalt oxide			
0.8 g	20	0.0011	0.9734
	40	0.001	0.9547
	60	0.0009	0.965
	80	0.0012	0.9864
(b) Modified cobalt oxide			
0.8 g	20	0.0011	0.9699
	40	0.0011	0.9488
	60	0.0009	0.9524
	80	0.0011	0.9831

tion rate constant) and time, respectively. The relationships between  $[\ln(C/C_0)]$  and irradiation time (reaction time) are as shown in Fig. 10a, b. It is obvious that there exists a linear relationship between  $[\ln(C/C_0)]$  and irradiation time. The pseudo-first-order rate constant  $k$  and linear regression coefficient ( $R^2$ ) for EB solutions with different initial EB concentrations are summarized in Table 4a, b, respectively.

According to the Langmuir–Hinshelwood model, the fact that the decrease of reaction rate constant with the increase of the initial concentration of EB solutions obtained from Table 4a, b could be explained as follows. The EB dye is first adsorbed on the surface of doped and pure cobalt oxide, and then the photocatalytic degradation takes place under mercury irradiation. With the increase of the initial EB concentrations, the EB molecules congregate on the surface of pure and doped cobalt oxide nanocatalysts. However, quenching

between these excited molecules irradiated by UV light will take place. The quenching probability could also increase with the increase of the initial EB concentrations. Consequently, the photocatalytic efficiency of pure and doped cobalt oxide nanocatalysts decreased with the increase of the initial eosine blue concentrations.

#### Reusability of photocatalyst

The stability of the pure and doped cobalt oxide catalysts was affirmed by reusability of the catalysts within the photocatalytic corruption of EB in UV–Vis illumination. To ponder its reusability, after photocatalytic debasement the powdered nanocatalyst was settled by gravity and after that was isolated. The recouped nanoparticles were collected and reused for three times beneath the same photocatalytic exploratory condition. Expulsion of EB by utilizing unadulterated cobalt oxide after first run accomplished 92%, second run 91.7%, third run 91.3% and fourth run 91% separately, whereas expulsion of EB by utilizing doped cobalt oxide after first run accomplished 95%, second run 94.7%, third run 94.5% and fourth run 94.2% individually as appeared within Fig. 11a, b. In this way, it is proposed that unadulterated and doped cobalt oxide nanocatalysts have way better solidness and does not appear noteworthy misfortune in movement after four cycles. It is found experimentally at each catalyst recycling the % degradation of EB dye was decrease due to reusability of the catalysts. It is recommended that immaculate and doped cobalt oxide catalysts do not get photoerode amid photocatalytic degradation [26].



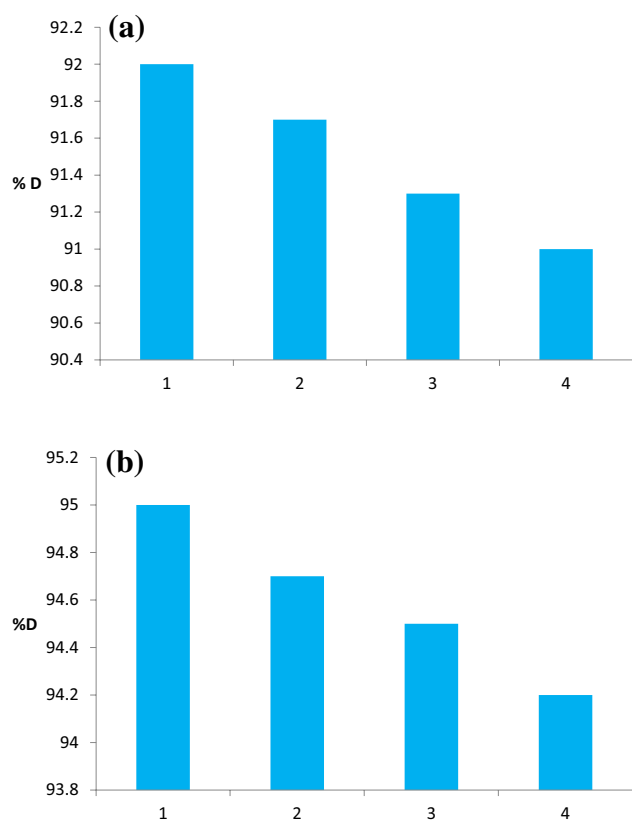


**Fig. 11** a Recycling performance of the pure cobalt oxide catalyst. b Recycling performance of the doped cobalt oxide catalyst

## Conclusions

Eosine blue dye is one of the major contaminants present in industrial wastewater. It enters the environment when released through wastewater and exerts detrimental effects on flora and fauna. The proposed nanoparticles are found to be useful for the wastewater purification. Both synthesised pure and doped cobalt oxide nanomaterials were successfully applied for the removal of eosine blue dye from an aqueous solution. The synthesised doped cobalt oxide nanoparticles have more efficiency for the degradation of eosine blue than pure cobalt oxide due to decrease in band gap. The degradation efficiency of both catalysts indicated that the low initial dye concentration and high catalyst dose are more favorable for the degradation process. The process obeys the pseudo-first-order kinetics with good correlation with linear regression coefficient. The experimental results of this study show that the doped cobalt oxide catalyst degrades eosine blue up to 95% while pure cobalt oxide degrades up to 92%. These nanocatalysts have great potentials to be used as water purification media,

where the potential of this material can be further modified to increase its degradation capacity towards targeted compounds.

**Acknowledgements** Authors gratefully acknowledge the SAIF, Chandigarh (Punjab University), for XRD and SAIF, NMU, Jalgaon, for SEM analysis. Authors are thankful for SAIF, IIT, Bombay, for TEM and EDX analysis. Authors are very thankful for Department of Chemistry, Pratap College, Amalner, Department of Chemistry, L. V. H. College, Panchavati, Nashik, and Nanochemistry Research Laboratory, G. T. P. College, Nandurbar, for providing necessary laboratory facilities.

**Open Access** This article is distributed under the terms of the Creative Commons Attribution 4.0 International License (<http://creativecommons.org/licenses/by/4.0/>), which permits unrestricted use, distribution, and reproduction in any medium, provided you give appropriate credit to the original author(s) and the source, provide a link to the Creative Commons license, and indicate if changes were made.

## References

- Patil, Manohar R., Shrivastava, V.S.: Photocatalytic degradation of carcinogenic methylene blue dye by using polyaniline-nickel ferrite nano-composite. *Der Chem Sin* **5**(2), 8–17 (2014)
- Guo, H., Ke, Y., Wang, D., Lin, K., Shen, R., Chen, J., Weng, W.: Efficient adsorption and photocatalytic degradation of Congo red on to hydrothermally synthesized NiS nanoparticles. *J Nanopart Res* **15**, 1475 (2013)
- Van Nguyen, C.: Bifunctional core-shell nanocomposite Mn doped ZnO/Fe<sub>3</sub>O<sub>4</sub> for photo degradation of reactive blue 198 dye. *Nanosci Nanotechnol* **5**, 035014-19 (2014)
- Vinodgopal, K.: Enhanced rates of photocatalytic degradation of an azodye using SnO TiO<sub>2</sub> coupled semiconductor thin films. *Environ Sci Technol* **29**, 841–845 (1995)
- Abo-Farha, S.A.: Photocatalytic degradation of monoazo and diazo dyes in wastewater on nanometre-sized TiO<sub>2</sub>. *Researcher* **2**(7), 1–20 (2010)
- Soltani, T., Entezari, M.H.: Solar photocatalytic degradation of RB5 by ferrite bismuth nanoparticles synthesized via ultrasound. *Ultrason Sonochem* **20**, 1245–1253 (2013)
- Wang, W.P., Kalck, S.P., Faria, I.L.: Visible light photo degradation of phenol on MWNT- TiO<sub>2</sub> composite catalyst a prepared by a modified Sol-gel method. *J Mol Catal A* **235**(1–2), 194–199 (2005)
- Marandi, R., Mahanpoor, K., Sharif, A.A.M., Olya, A.E., Moradi, R.: Photocatalytic degradation of azo dye acid yellow 23 in water using NiFe<sub>2</sub>O<sub>4</sub> nanoparticles supported on clinoptilolite as a catalyst in a circulating fluidized bed reactor. *J Basic Appl Sci Res* **3**(5), 347–357 (2013)
- Joshi, K.M., Patil, B.N., Shirsath, D.S., Shrivastava, V.S.: Photocatalytic removal of Ni (II) and Cu (II) by using different semiconducting materials. *Adv Appl Sci Res* **2**(3), 445–454 (2011)
- Kulkarni, M., Thakur, P.: Photocatalytic degradation and mineralization of reactive textile azo dye using semiconductor metal oxide nano particles. *Int J Eng Res Gen Sci* **2**(2), 245–254 (2014)
- Hankare, P.P., Jadhav, A.V., Patil, R.P., Garadkar, K.M., Mulla, I.S., Sasikala, R.: Photocatalytic degradation of rose bengal in visible light with Cr substituted MnFe<sub>2</sub>O<sub>4</sub> ferrosin. *Arch Phys Res* **3**(4), 269–276 (2012)
- Roy, T.K., Mondal, N.K.: Photocatalytic degradation of congo red dye on thermally activated zinc oxide. *Int J Sci Res Environ Sci* **2**(12), 457–469 (2014)

13. Zhao, H., Tian, F., Wang, R., Chen, R.: A review on bismuth related nanomaterials for photocatalysis. *Rev Adv Sci Eng* **3**, 3–27 (2014)
14. Stella, C., Soundararajan, N., Ramachandran, K.: Chunk shaped ZnO/Co<sub>3</sub>O<sub>4</sub> nanocomposite for ethanol sensor. *Adv Mater Lett* **7**(8), 652–658 (2016)
15. Adekunle, A.S., Ozoemena, K.I.: Comparative surface electrochemistry of Co and Co<sub>3</sub>O<sub>4</sub> nanoparticles: nitrite as an analytical probe. *Int J Electrochem Sci* **5**, 1972–1983 (2010)
16. Faraji, M., Yamini, Y., Rezaee, M.: Magnetic nanoparticles: synthesis, stabilization, functionalization, characterization, and applications. *Iran Chem Soc* **7**(1), 1–37 (2010)
17. Mondal, A., Mondal, A., Adhikary, B., Mukherjee, D.K.: Cobalt nanoparticles as reusable catalysts for reduction of 4-nitrophenol under mild conditions. *Bull Mater Sci* **40**(2), 321–328 (2017)
18. Azhdari, F., Ghaz, M.M.: Photocatalytic degradation of textile dye direct orange 26 by using CoFe<sub>2</sub>O<sub>4</sub>/Ag<sub>2</sub>O. *Adv Environ Technol* **2**, 77–84 (2016)
19. El-Bahy, Z.M., Mohamed, M.M., Zidan, F.I., Thabet, M.S.: Photo-degradation of acid green dye over Co–ZSM-5 catalysts prepared by incipient wetness impregnation technique. *J Hazard Mater* **153**, 364–371 (2008)
20. Narde, S.B., Lanjewar, R.B., Gadegone, S.M., Lanjewar, M.R.: Photocatalytic degradation of azo dye congo red using Ni<sub>0.6</sub>Co<sub>0.4</sub>Fe<sub>2</sub>O<sub>4</sub> as photocatalyst. *Der Pharma Chem* **9**(7), 115–120 (2017)
21. Sharma, O., Sharma, M.K.: Use of cobalt hexacyanoferrate (II) semiconductor in photocatalytic degradation of neutral red dye. *Int J ChemTech Res* **5**(4), 1615–1622 (2013)
22. Mukhtar, M., Munisa, L., Saleh, R.: Co-precipitation synthesis and characterization of nanocrystalline zinc oxide particles doped with Cu<sup>2+</sup> ions. *Mater Sci Appl* **3**, 543–551 (2012)
23. Esquivel, K., Garc, M.G., Rodr, F.J., Ortiz-Frade, L.A., Godinez, L.A.: Study of the photo-electrochemical activity of cobalt- and nickel-doped TiO<sub>2</sub> photo-anodes for the treatment of a dye-contaminated aqueous solution. *J Appl Electrochem* **43**, 433–440 (2013)
24. Sharma, A., Lee, B.K.: Adsorption/photocatalytic process for naphthalene removal from aqueous media using in situ nickel doped titanium nanocomposite. *J Environ Manag* **155**, 144–152 (2015)
25. Khairnar, S.D., Patil, M.R., Shrivastava, V.S.: Hydrothermally synthesized nanocrystalline Nb<sub>2</sub>O<sub>5</sub> and its visible light photocatalytic activity for the degradation of Congo-red and methylene blue. *Iran J Catal* **8**(2), 143–150 (2018)
26. Patil, S.P., Patil, R.P., Mahajan, V.K., Sonawane, G.H., Shrivastava, V.S.: Facile sonochemical synthesis of BiOBr-graphene oxide nanocomposite with enhanced photocatalytic activity for the degradation of direct green. *Mater Sci Semicond Process* **52**, 55–61 (2016)

**Publisher's Note** Springer Nature remains neutral with regard to jurisdictional claims in published maps and institutional affiliations.

